Sci. J. Fac. Sci. Menoufia Univ. Vol. VIII (1994) 205-229

MINERALOGICAL AND GEOCHEMICAL STUDIES ON THE RECENT NILE SEIMENTS OF THE AREA BETWEEN THE OLD ASWAN DAM AND HIGH DAM

MOHAMMED ELDARDIR

National Inst. Oceanography and
Fisheries, Egypt.

ABSTRACT

Thirty core subsurface sedimentary samples of the recent Nile sediments between the old Aswan Dam and High Dam were colected from 3 sites and analyzed mechanically, mineralogically and chemically.

The clay fraction forms the main bulk of the studied sediments while the sand fraction constitutes less than 10%.

The sediments are mainly affected by early diagenetic processes as indicated by the absence of aragonite in the middle and base parts of the cores. The composition of clay minerals show that the River Nile played the principle role for supplying the bottom sediments in the studied area. The country rocks can not be excluded.

Geochemical analysis of the sediments shows that the distribution of the chemical constituents are controlled by fluvial sedimentation, mineral constituents and pH of the water.

The aqueous migration coeffecient values (K_X) for the elements in the fresh water of the studied part arranged in a decreasing order of abundance are as follows: Ca, Mg, (Na-K) Mn, Si and Fe.

INTRODUCTION

The studied part of the River Nile lies between the old Aswan Dam and High Dam (Fig. 1) and was formed on the River Nile at Aswan area after the consturction of the High Dam.

The geologic rock units exposed in this area on both eastern and western banks of the Nile are represented by Aswan granites, the sandstone of the Nubia facies and the Quaternary old Nile sediments.

As a matter of fact no work has been undertaken on the recent Nile sediments in the investigated part between old recent Nile sediments in the investigated part between old Aswan Dam and the High Dam.

MATERIALS AND METHODS

During september 1992, thirty samples were collected using core-samples from 3 sites namely from north to south: I, II, and III parts (Fig 1). From each core, 10 sampler were taken every 5 cms.

The samples were mechanically analysed using sieving and settling techniques. Nine selected bulk samples were subjected to X-ray diffraction analysis using Shimadzu diffractometer (type XD-3). The fraction (<2μ) of six samples representing the the core sediments were also investigated to identify the clay minerals. Three X-ray diffraction patterns were recorded for each oriented specimen, viz in the untreated state, after glycolation and after heating to 550 °C for 2 hours. Peak intensities were calculated by multiplying peak high by width at half high. In order to calculate the semi-quantitative mineral composition, peak intensities of kaolinite (7A°), illite (10A°) and smectite (14 A°) were multiplied by factors of 2,4 and 1 respectively (Biscay 1963).

The chemical contents of the studied sediments were estimated gravimetrically by perkin-Elmer Atomic Absorption Spectrophotometer and Flame photometer techniques. The estimation of organic matter was carried out as described by Hanna (1965).

The water samples wer collected (at the site of cores) using Van Dorn bottle at 3 levels and were examined for pH and total dissolved salt (T.D.S). They were chemically analysed for Ca, Mg, K, Cl, Fe, Mn and SiO2 according to procedures described by the American Public Health Association (APHA) (1980).

GRAIN SIZE

The grain size analysis revealed that the sand fraction constitutes less than 10% of the samples from 3 studied cores while the silt ranges from 40% to 45%. The clay fraction forms the main size of the studied sediments (45-50%) (Fig. 2).

MINERALOGY

Bulk Samples:

The X-ray diffraction analysis of the representative core samples show that the detected minerals are: Quartz, kaolinite, illite, aragonite, calcite, hematite, rutile and sphene (Fig. 3, Table 1)

From the lateral and vertical distribution of the minerals it is found that quartz and kaolinite are detected in the core sediments at different depths, calcite is not detected in the sample sediments at the surfaces parts, aragonite proved to appear in the surface sediments, sphene was not recorded in sediments of the southern part (core III). Rutile is detected in core III sediments, illite is recorded in the northern and southern parts (core I and core III respectively). It is absent in core II sediments (Middle part).

Rankama and Sahama (1954) stated that fresh water shells are mostly aragonite. The presence of aragonite could be related to the aragonite shells of generally more stable and sometimes surviving to old diagenetic process (Kukal 1971). The aragonite eventually undergoes recrystallization to calcite (Deer et al. 1978). In the present study the absence of aragonite in the middle and base parts of the cores may be attributed to an early diagenetic processes changing it to calcite.

In the present study rutile, hematite and sphene are found as detrital grains. The absence of these minerals in the basal parts of the 3 cores (samples No. 10,20 and 30) can be explained as due to the increase of size of the sand grains(>500mm).

Clay minerals:

Table (2) shows the semi-quantitative composition of the analyzed samples and typical X-ray diffraction pattern is shown in fig. 4. all samples contain smectite, illite and kaolinite with relative content ranging between (1.36-90.24%), 2.81-65.70% and 4.32-32.87%) respectively (Table 2).

Smectite, illite and kaolinite are considered as detrital particle transported from source area and were deposited without any diagenetic changes (Pryor and Glass, 1961).

The identified clay minerals in the studied samples do no differ from those detected in the previous studies carried out on Lake Nasser sediments (Hassan et al.; 1977 and Ahmed et al.;

1993). However the frequency of illite is relatively higher than kaolinite, a result which disagrees with the finding of Hassan et al.; 1977 and Ahmed et al.; 1993. In the present work the River Nile played the principle role for supplying the bottom sediments. The country rocks (Aswan granites and the sandstone of the Nubia facies) can not be excluded. The abundance of smectite is probably affected by the pH value, (7.33-8) which is recorded in the water (Table 4)

GEOCHEMISTRY

The values of the analysed chemical constituents forming the studied sediments are given in table (3).

The sediments of core I contain low SiO_2, Al_2O_3, MnO_2, K_2O and MgO values and contain more Fe_2O_3, TiO_2, C_aO, Na_2O, P_2O_5, Cl and So_3 values relative to core II and core III sediments (table 3)

The chemical constituents in the studied samples show narrow range of values with the exception of GaO in the sediments of cores II and III (Table 1). On the other hand the distribution curves show the increase of M_gO and K_2O contents with depth. The curves of the other constituents do not show particular trend (Fig. 5)

Al_2O_3 content varies inversely with increase of SiO2 content due to increase of the sand size amount (Fig. 5). This may be attributed to increase of amount of free quartz. However Aluminum oxide remains dissolved both in acid solution with pH less than 4 and in basic waters (pH.) (Mason, 1966). Aluminum oxide hydrate precipitates in the neghbourhood of the neutral point which is recorded in the water of the investigated area, its pH value ranges from 7.42 to 8.0 (Table 4).

Al_2O_3 and Fe_2O_3 show consistent vertical distribution specially in core II and core III sediments (Fig.5). The scatter plot diagram and the correlation coeffecient values (Fig.6) manifested such relation for sediments of cores II and III. This suggests their deposition as hydrolysates. Both element oxides show similar ionic potential values (Mason 1966). However in those of core I insignificant relation of Al_2O_3 and Fe_2O_3 suggests their independent behaviour. This may be explained by the increase of the clay fraction amount at the expense of sand fraction (Fig. 7). The abundance of Fe_2O_3 in the studied sediments reflects the presence of free hydrate iron oxides as well as iron minerals in the core sediments. TiO_2 content ranges from 1.89% (sample No. 21) to 2.60% (S.N 10) (Table 3). Both iron and titanium oxides show consistent distribution with each other (Fig. 8). This favours its deposition as hydrolysate. Moreover, the X-ray diffraction analysis revealed the presence of sphene and rutile in some analysed samples. However both inconsistent oxides in the sediments of core II show inconsistent distribution (correlation coefficients= 0.065). Mean while TiO_2 is correlated with SiO_2 (Fig 9) (r= 0.66) which is significant at P= 95%. This suggests that it occurs in another phases most probably silicate (sphene).

MnO ranges from 0.089% to 0.101% (Table 3). Core III sediments contain the highest percentage (0.101) in comparison with core I and core II sediments.

CaO ranges from 3.31% (S.N. 18) to 5.62% (S.N. 12) (Table 3). Core I sediments show significant positive correlation (r= 0.76) o Al_2O_3 vs. CaO (Fig 10). This supports the abundance of CaO in aluminum silicate minerals (plagioclase). In the sediments of core II and core III, calcium oxide is present most probably in the form of carbonates due to the significant negative correlation between CaO and Al_2O_3 (Fig. 10). MgO ranges from 1.85% (S.N. 2) to 2.34% (S.N. 16). Core II sediments show the highest Mg content (2.34%) in comparison with core I sediments containing the lowest percentage (1.85) (Table 3).

Worth of remark that MgO is independent on CaO as favoured from the negative correlation value (Fig. 11).

Na_2O ranges between 0.43% (S.N. 26) and 1.63% (S.N. 20) Core II sediment contain the high percentage of Na_2O (1.63) whereas the lowest percentage (0.43) is recorded in core III sediments. K_2O ranges from 1.32% (core I & III) to 1.53% (core II). (Table 3) Na_2O and K_2O vertical variation curves (Fig.5) show mostly consistent distribution with each other and with those of SiO_2 with the exception of those of core I sediments show slight variation in the content of SiO_2.They are distinguished with the highest clay fraction amount. These consistent distribution favours their occurrance as silicate minerals mostly feldspars.

P_2O_5 varies from 0.211% (S.N 18) to 0.313% (S.N 28) (Table 3). The highest content of P_2O_5 is recorded in core III sediments whereas the lowest is recorded in core II sediments. Organic matter varies between 0.80% (S.N. 11) to 1.31% (S.N. 21). Core III sediments have the highest amount (1.31%) whereas core II sediments contain the lowest amount (0.80%) (Table 3). The independent relationship between P_2O_5 and organic matter supports the idea that P is not only of organic origin but also of inorganic origin. The vertical distribution curves of P_2O_5 and CaO (Fig. 5) are mosly consistent with each other in the sediments of cores II and III while in core I sediments the relation is not obvious. This may favour its biogenic origin.

SO_3 ranges from 0.083% (S.N. 20) to 0.255 (S.N. 7). The highest amount 0.255%) is recorded in core I sediments. The vertical variation curves as well as the plots of SO_3 versus CaO (Figs. 5,12) show the presence of positive correlation between the two components in the sediments of core II while it is not obvious in the sediments of cores I and III. This reflects the presence of SO_3 as detrital gypsum in the core II sediments.

AQUEOUS MIGRATION OF CHEMICAL COMPONENTS

Nine water samples were analyzed at several levels of water (Table 4). To characterize the intensity of aqueous migration of elements, Perelman (1968) introduced the aqueous migration coefficient (K_x), which can be computed according to the following equation.

$$K_X = \frac{m_x 100}{an_x}$$

m_X = content of the element x in water (mg/1).

n_X = content of the element x in rock (%).

a = total dissolved salts in water (mg/1).

He found that Ca, Na, Mg are strong migrated elements in both oxidizing and reducing conditions as their K_X value ranges between 1 and 10.. K_X values of Ca, Mg, Na, K, Mn, Si, and Fe in the Nile water at 3 depths of the area under investigation were calculated (Table 5). The average content of these elements in the lithosphere given by Vinogradov (1962) is taken to represent n_X in the equation. This is because the catchment area of the Nile river occupies large territories of the Central and Eastern Africa where the various known rock units of the Arab Nubian shield are outcropping.

According to the calculated values of K_X, the element arranged in a decreasing order of K_X values are as follows: Ca, Mg, (Na-K) Mn, Si and Fe.

However, K_X value increases with increase of depth of water as it is the highest in the bottom water while the least in the surface water. This can be understood in terms of pH values (Table 4) where its K_X low values are present in the relatively basic water.

CONCLUSIONS

The sediments deposited in the area under study are sand, silt and clay given in an increasing order of abundance. These fractions show narrow range of variability both laterally and vertically.

The sediments are mainly affected by early diagenetic processes as indicated by the absence of aragonite in the middle and base parts of the cores. Clay minerals composition show that the River Nile played the principle role of supplying the bottom sediments in the studied area. The country rocks are not excluded.

The changes in the chemical composition favour that fluvial sedimentation, mineral constituent, pH of the water are the effective processes in the deposition of the chemical elements.

The aqueous migration coeffecient values (K_X) for the elements in the fresh water of the studied area arranged in a decreasing order are of abundance as follows: Ca, Mg, (Na-K), Mn, Si and Fe.

REFERENCES

Ahmed, E.A., El Dardir, M. and Gindy, N.N (1993): Sedimentological, mineralogical and geochemical studies on some recent khors sediments, Lake Nasser, Egypt. Jour. African Earth Sci. Vol. 17, No 3.pp. 383-397.

Amircan Public Health Association (APHA) (1980): Standard Methods for the examination of water and waste water 15 th end. New Yourk, U.S.A.

Biscay, B.E. (1965): Mineralogy and sedimentation of deep sea clays in the Atlantic and adjacent seas and oceans. Bull Geol. Soc.. Am. 76:803-822).

Deer, A.W., Howie, A.R., and Zussman, J. (1978): An introduction of the rock-forming minerals, Longman Group Ltd., London, 528 p. Hanna, A. (1965): Organic matter in soil. In: Chemistry of Soil E.E. Bear. (Ed). Amer. Chem. Soc. Monograph series 515 p. .

Hassan, F., Abu Zeid, M. and Hafez, K. (1977): Mineralogical composition of the clay fraction of the High Dam Lake Sediments. Lake Nasser and River Nile Project. Report prepared for the Acad. of Sci. Res. and Tech. Egypt. 17 p.

Kukal, Z. (1971): Geology of Recent sediments Academic press, London 490 p.

Masson, B, (1966): Principles of Geochemistry 3rd ed New York. 329 p.

Pryor, W.A. and Glass, H.D. (1961): Cretaceous- Tertiary clay mineralogy of the Upper Mississippi embayment. Jour. Sed. Petrology, 31, 38-51.

Perelman. A.I. (1968): Geochemistry of epigenetic processes (Supergene zone) M.. Nerda (In Russian).

Rankama, K., and Sahama, T.G., (1954): Geochemistry Chicago, Univ.Chicago press, XVI, 912 pp.

Vingordov, A.P. (1962): Average content of chemical elements in the main types of igneous rocks of the earth, crust, Geochemistry No. 7.

Table 1. Lateral and vertical variation in the mineral composition of the core sediments.

Core No.	Sample No.	Minerals
I	1	Quartz, kaolinite, illite, aragonite, sphene.
	5	Quartz, kaolinite, illite, hematite, calcite.
	10	Quartz, kaolinite, aragonite, calcite.
II	11	Quartz, kaolinite, aragonite, hematite, sphene.
	15	Quartz, kaolinite, aragonite, calcite, sphene.
	20	Kaolinite, quartz, calcite.
III	21	Quartz, kaolinite, rutile, aragonite.
	25	Quartz, kaolinite, illite, hematite, rutile.
	30	Quartz, kaolinite, calcite.

Table 2: Relative abundance frequencies of clay minerals (%) in the studied sediments.

Mineral Sample No.	Smectite	Illite	Kaolinite
1	1.36	65.70	32.87
10	81.35	13.55	5.08
11	39.40	33.93	26.50
20	7.27	63.63	29.00
21	90.21	2.81	6.97
30	90.24	5.43	4.32

Table :3 Results of chemical analysis of sediments collected from the area.

Sample No.	SiO_2	Al_2O_3	Fe_2O_3	TiO_2	MnO	CaO	MgO	Na_2O	K_2O	P_2O_5	Cl	Organic matter	SO_3	H_2O	
1	49.2	15.3	10.33	2.54	0.092	5 02	1.86	1.02	1 41	0.282	0.008	1.19	0 137	12 7	Top
2	49 0.	15.3	10.33	2.55	0.091	5.02	1.85	1.02	1.4	0.28	0.008	1.2	0.13	12.7	
3	49 0	15.31	10.2	2.55	0 09	5 01	1.86	1 02	1.39	0.277	0.009	1.2	0.125	12.72	
4	48 65	15 54	10 14	2 59	0.089	5 02	2 33	1 05	1.32	0.267	0 01	0 9	0 25	12 76	
5	49.1	15 2	10 17	2 59	0 089	4.95	1.95	0 89	1.4	0.278	0.009	0 92	0.136	12.7	Core I
6	49.21	15.13	10.19	2.55	0.089	4.89	1.99	0 86	1.42	0.289	0.008	0.91	0 19	12.68	
7	49.2	15.1	9.7	2.32	0.09	4 9	2.1	1.63	1.42	0.277	0.008	0.92	0.255	12 69	
8	49.04	15.16	9.66	2.32	0.094	5.03	2.19	1.52	1.42	0.275	0.009	0.92	0.235	12.95	
9	49.15	15.12	10.3	2.54	0.091	4.95	2.09	1.2	1.4	0.274	0.01	0.89	0.122	12.81	
10	49.18	15.00	10 42	2.6	0.091	4.84	2.07	1.19	1.36	0.274	0.01	0.9	0.12	12.8	Base
11	51.9	14.00	9.57	2.228	0.099	5.6	1.93	1.3	1.53	0.27	0.008	0.8	0.19	11.2	Top
12	51.6	14 19	9 63	2.17	0.099	5.62	1.97	1.27	1.51	0.284	0.006	0.97	0.185	11.4	
13	49.5	15.5	10.7	2.2	0.098	3.75	2.0	0.87	1.37	0.25	0.006	0.98	0 105	12.5	
14	48 84	16.24	10.7	2.24	0.099	3 65	2.05	0.79	1.48	0.217	0.007	0.99	0.099	13 5	
15	51 75	15 2	9.86	2.28	0 095	4 05	2.21	1.15	1 43	0 28	0.007	0 9	0.099	11 7	Core II
16	52.9	14 48	9 85	2.20	0 094	4 53	2 34	1.23	1 43	0.302	0.007	1.0	0 121	10 35	
17	50.05	16 00	10.00	2.15	0.094	3.75	2.1	0.97	1.38	0.285	0.006	0.95	0.112	12.12	
18	49 09	16.63	10.18	1.99	0.094	3.31	1.94	0.82	1.38	0.211	0.007	0.95	0.095	14.2	
19	49.1	15.91	9.7	2.05	0.089	3.65	2.1	1.0	1.39	0.235	0.006	0.9	0.09	14.0	
20	52.46	14.03	9.4	2.5	0.089	4.76	2.32	1.63	1.41	0.285	0.006	0.85	0.083	11.2	Base
21	52 86	15.47	9.17	1.89	0.101	3.54	2.22	0 89	1.47	0.253	0.007	1.31	0.228	11 8	Top
22	52 9	15.3	9 2	1 97	0.1	3.7	2.1	0.9	1.46	0.257	0.008	1.3	0.226	11 5	
23	53 12	14.1	9.2	1.98	0 1	5.05	2.09	1.1	1.48	0.300	0.007	1.27	0.226	11.1	
24	53.12	14.12	9.31	2.06	0 099	5.02	2.06	1.12	1.48	0.303	0.009	1.12	0.1	11.09	
25	48 7	16.5	10.3	2.21	0 097	4.0	2.0	0.5	1.43	0.303	0.008	1.17	0.095	13 3	Core III
26	48.38	16.81	10 35	2.32	0.098	3.85	2.01	0.43	1.41	0.249	0.009	1.3	0 105	13.92	
27	48.9	15 85	9.85	2.45	0.095	5 1	2.03	1.1	1.32	0.269	0.008	1.2	0.115	12.1	
28	51.51	14.82	9.48	2.45	0 093	5 56	2 09	1.21	1.39	0.313	0.007	1.0	0.175	10 89	
29	50.5	15.75	10.00	2.25	0.099	3 81	2.06	1.09	1.4	0.27	0.007	1.3	0.092	11 9	
30	48 54	16.63	10.29	2.36	0.094	3.85	2.06	1.04	1.43	0.234	0.007	1.35	0.1	13.1	Base

Table 4. The chemical constituents (mg/l), total dissolved salts (mg/l) and pH values of the analysed water samples.

Core No.	Total depth (m)	Level	T.D.S	pH	Ca^{++}	Mg^{++}	Na^{+}	K^{+}	Cl^{-}	Fe	Mn	SiO_2
I	20	Surface	160	7.78	25.70	12.7	7.55	3.7	5.20	0.05	0.04	2.21
		Middle	160	7.73	24.70	9.0	12.70	4.1	5.21	0.12	0.08	1.20
		Bottom	151	7.94	24.00	9.3	17.90	3.9	5.00	0.73	0.09	1.33
II	12	Surface	163	7.33	27.75	12.5	7.50	3.8	5.30	0.04	0.05	2.70
		Middle	160	7.49	27.00	8.7	12.50	4.2	5.31	0.12	0.07	1.30
		Bottom	154	7.42	26.40	9.0	17.70	3.9	5.75	0.070	0.09	1.23
III	10	Surface	162	8.00	27.25	12.65	7.56	3.5	5.77	0.05	0.05	2.50
		Middle	168	7.51	26.35	9.24	13.98	4.5	5.27	0.15	0.08	1.25
		Bottom	155	7.82	26.45	9.24	18.90	4.0	5.75	0.075	0.10	1.25

Table 5. Aqueous migration coefficient K_x of Na, Ca, Mg, K, Mn, Si and Fe.

Core No.	Total depth (m)	Level	Ca	Mg	Na	K	Mn	Si	Fe
I	20	Surface	5.87	1.88	0.93	0.93	0.25	0.022	0.006
		Middle	2.08	3.18	1.03	1.03	0.50	0.012	0.016
		Bottom	5.37	4.74	1.03	1.03	0.59	0.030	0.010
II	12	Surface	5.75	4.10	0.51	0.51	0.31	0.056	0.005
		Middle	4.17	2.90	1.05	1.05	0.44	0.028	0.018
		Bottom	5.79	3.12	1.01	1.01	0.58	0.027	0.010
IIII	10	Surface	5.68	4.17	0.86	0.86	0.31	0.052	0.007
		Middle	5.30	2.94	1.07	1.07	0.47	0.025	0.020
		Bottom	5.77	3.19	1.03	1.03	0.64	0.027	0.010

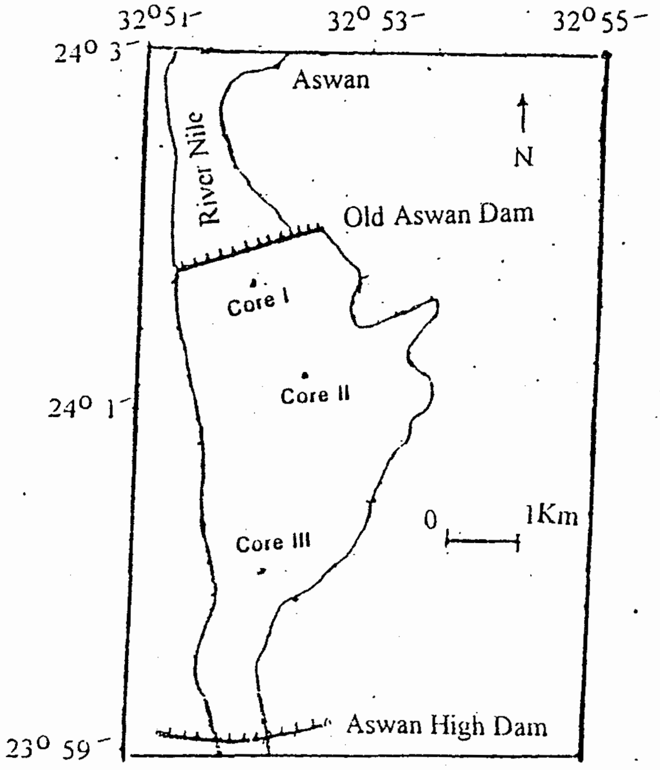

Fig. 1 Key map showing locations of the studied cores.

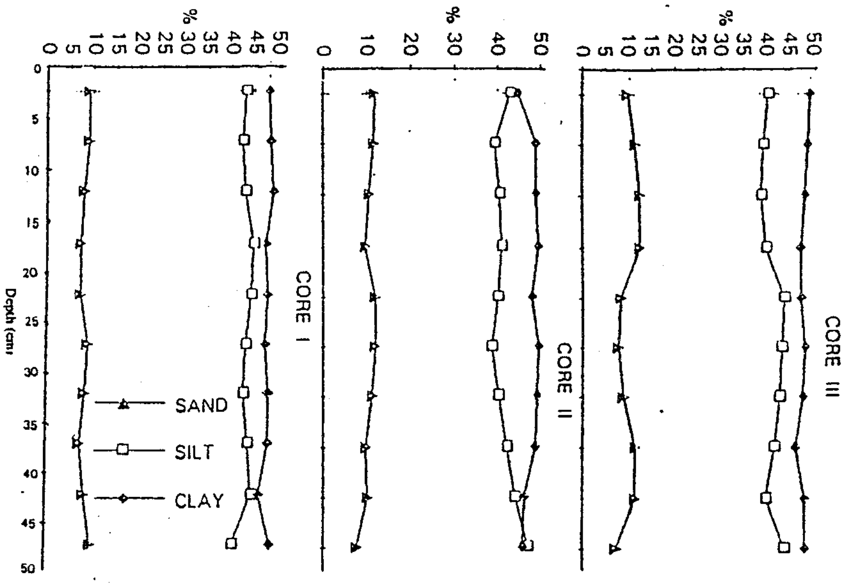

Fig. 2. Vertical distribution of grain size composition.

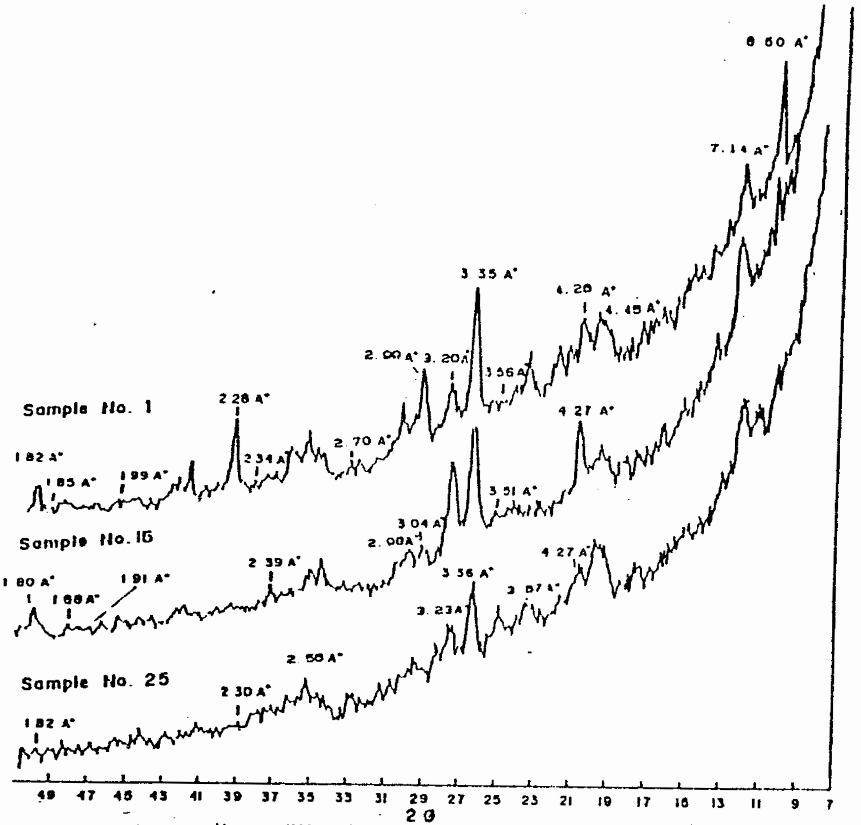

Fig. 3. X-ray diffraction patteerns of bulk samples

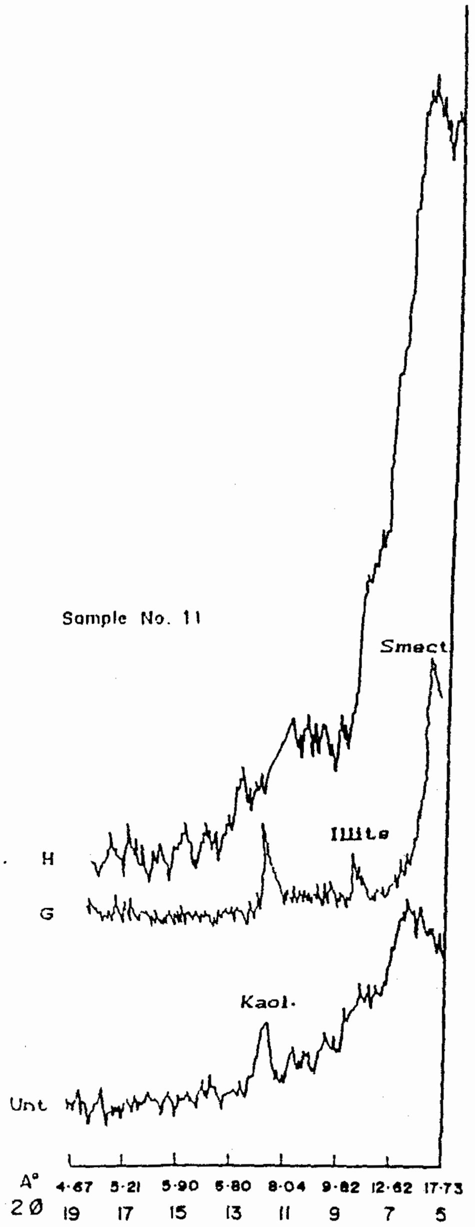

Fig. 4. X-ray diffraction pattern of clay fraction.

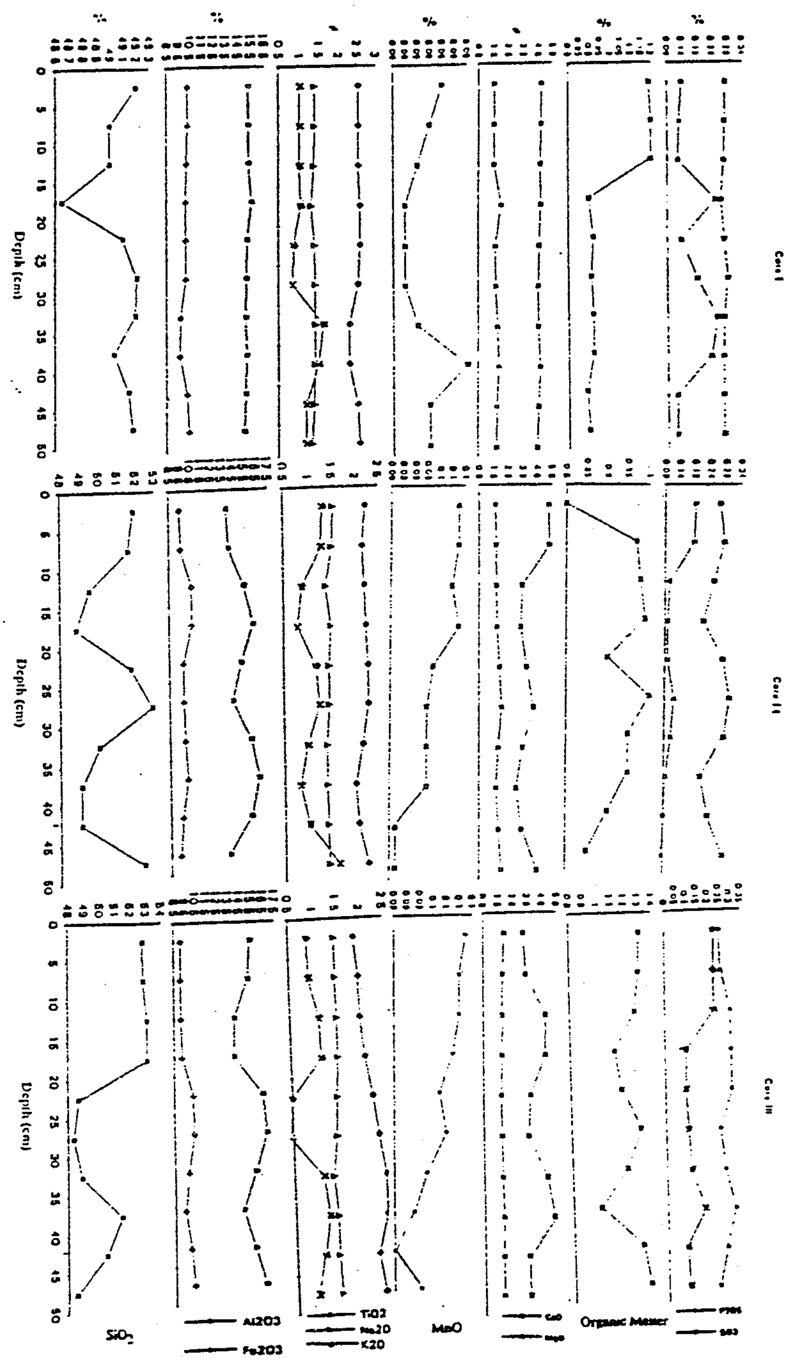

Fig. 5. Vertical distribution of chemical constituents.

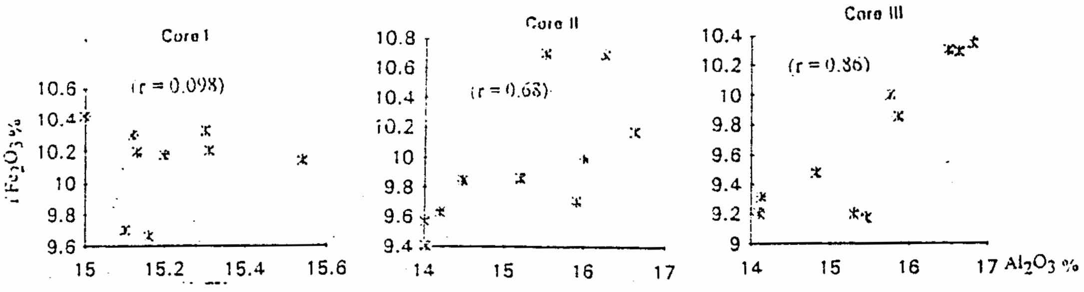

Fig. 6. Scatter diagram of Al_2O_3 vs. Fe_2O_3 in the core sediments.

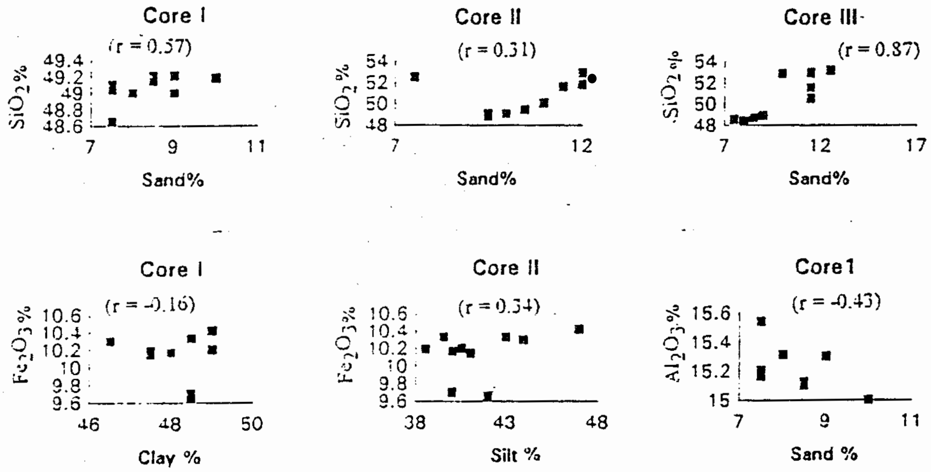

Fig. 7. Scatter diagram of sand fraction vs. SiO_2 and clay, silt and sand fraction vs. Fe_2O_3 vs. and Al_2O_3.

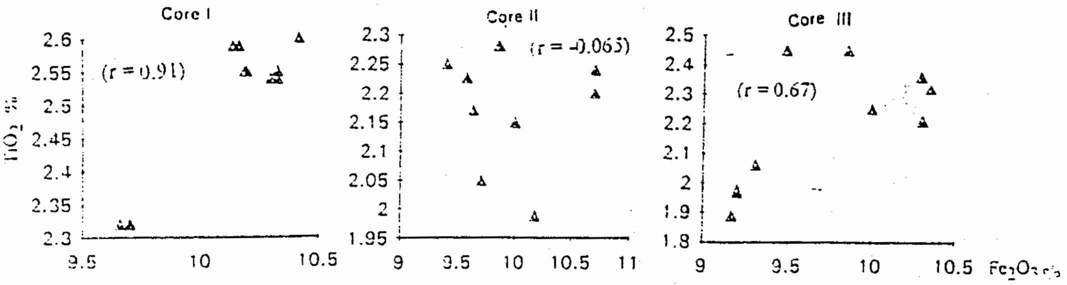

Fig. 8. Scatter diagram of Fe_2O_3 vs. TiO_2 in the core sediments.

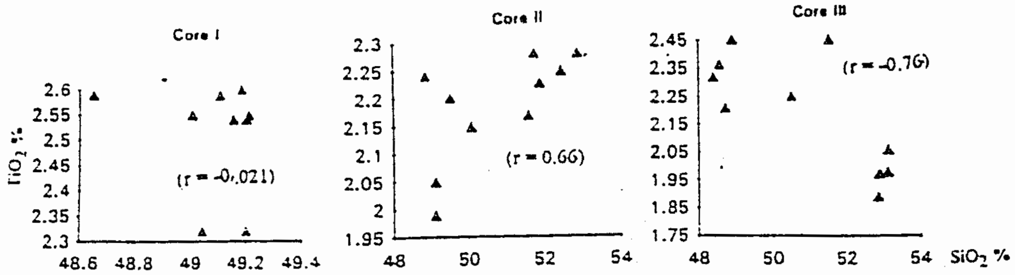

Fig. 9. Scatter diagram of SiO_2 vs. TiO_2 in the studied sediments

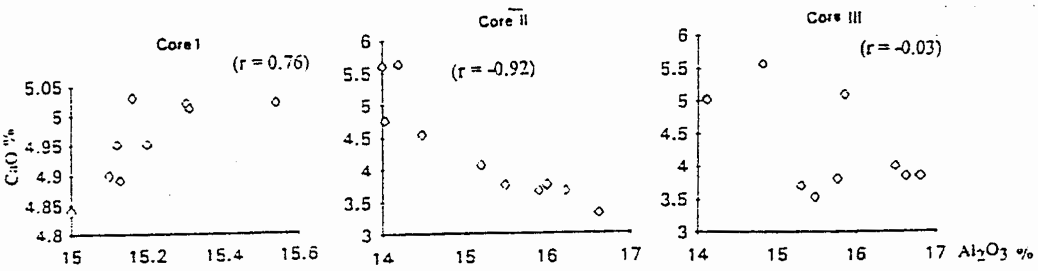

Fig. 10. Scatter diagram of Al_2O_3 vs. CaO in the core sediments

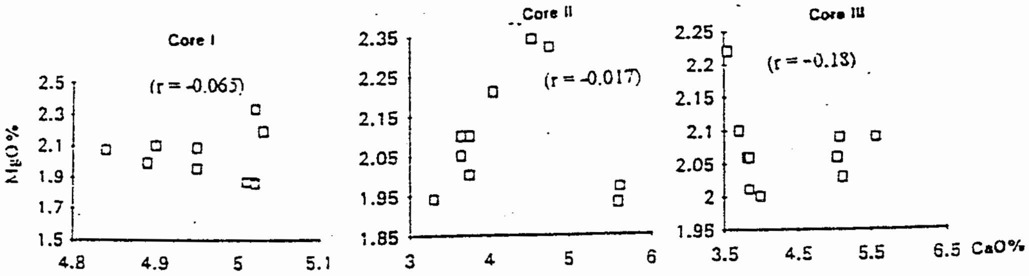

Fig. 11. Scatter diagram of CaO vs. MgO in the core sediments

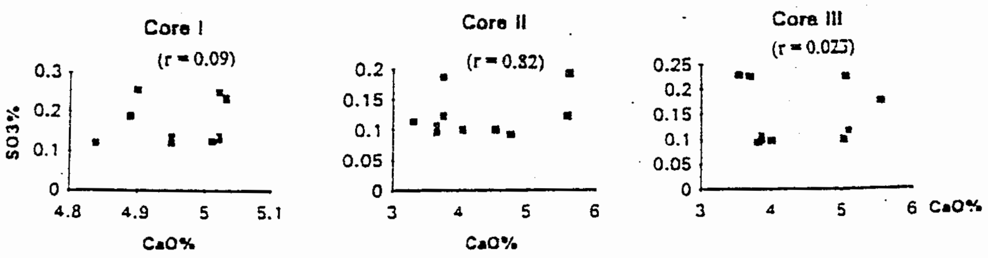

Fig. 12-Scattered diagram of CaO vs. SO_3 in the studied sediments

دراسات معدنية وجيوكيميائية لرواسب النيل الحديثة فى المنطقة بين السد العالى وخزان أسوان

محمد الدردير محمد على

المعهد القومى لعلوم البحار والمصايد – مصر

يتضمن البحث تحليل عدد ٣٠ عينة أسطوانية أخذت من ثلاثة مواقع وقد حللت العينات تحليلا ميكانيكيا ومعدنيا وكيميائيا لتحديد مكوناتها الرئيسية والغير رئيسية.

دلت الدراسة الميكانيكية على أن حجم الطين هو المكون الأساسى لهذه الرواسب يليه السلت ثم الرمل.

وتشير الدراسة المعدنية أن الرواسب قد تاثرت بمرحلة تغير مبكر ويدل على ذلك إختفاء معدن الاراجونيت فى المناطق المتوسطه والسفلى من القطاعات بينما يظهر هذا المعدن فى الأجزاء العليا، وتفيد الدراسة ايضا أن مياه النيل تلعب دورا رئيسيا فى إمداد الرواسب بمعادن الطين.

وقد دل التحليل الجيوكيميائى أن توزيع المكونات مرتبط بالترسيب النهرى والمكونات المعدنية بالإضافة إلى الأس الهيدروجينى.